Interference in reflected second-harmonic generation from thin nonlinear films

M.S. Yeganeh, J. Qi, J. P. Culver, and A.G. Yodh
Department of Physics, University of Pennsylvania, Philadelphia, Pennsylvania 19104

M.C. Tamargo
Bellcore, 331 Newman Springs Road, Red Bank, New Jersey 07701
(Received 6 November 1991; revised manuscript received 23 January 1992)

We have observed interference in reflected second-harmonic generation from two adjoined nonlinear slabs. Experimental results on ZnSe/GaAs(001) heterostructures are obtained and compared to theoretical calculations of the phenomena. Together, the experiments and calculations enable us to deduce the frequency-dependent bulk nonlinear susceptibility for ZnSe near the E_0 transition.

I. INTRODUCTION

Although interference in reflection from thin multilayered dielectric films is an important and well-understood phenomenon in linear optics,[1] the analogous problem in nonlinear optics is not well studied. Nearly 30 years ago Bloembergen and co-workers introduced electromagnetic nonlinearities into Maxwell's equations and derived the conditions for reflection and refraction at the surfaces of nonlinear dielectrics.[2] They showed that the solution of Maxwell's equations with the proper boundary conditions leads to the production of harmonic waves in reflection and transmission. The most widely studied *interference* phenomenon in nonlinear optics was connected with the generation of harmonics in transmission through a single nonlinear slab. Under these conditions one observes Maker fringes.[3,4] These fringes arise because the source polarization and the free wave generated by this polarization have different phase velocities. Interference in harmonic generation has also been observed in other contexts. For example the phase shift between substrate and adsorbate nonlinearities has been seen in several systems,[5] and interference between monolayers on opposite sides of a single glass substrate has been observed in harmonic generation as a function of slide orientation.[6] In this paper we investigate a class of nonlinear optical interference phenomena that is more akin to linear reflection from a dielectric mirror. In particular, we observe interference in the production of second-harmonic (SH) waves as a result of reflection from two adjoined nonlinear optical slabs. This problem is similar to the Maker fringe phenomenon, since SH generation accompanies the transmission of the fundamental field over large distances, but we shall see that the second nonlinear slab introduces further complexities.

Besides its intrinsic interest, interference in harmonic generation from thin nonlinear films is important for other reasons. For example, the phenomenon provides a methodology for measuring the second-order susceptibility of thin overlayer materials. Since many unusual crystalline materials can only be grown in very thin layers above other high-quality solids,[7] the ability to measure nonlinearities in composite systems is valuable. In addition, as the use of three-wave mixing to probe solid interfaces grows,[8–12] it becomes essential to understand fully how interference phenomena can affect the intensity of these signals.

We have observed interference in reflected second-harmonic generation (SHG) from a series of ZnSe/GaAs(001) heterostructures with varying overlayer thickness. A theoretical solution of the problem is presented, and used to analyze our measurements. Several existing theoretical schemes can be applied to arrive at a solution to this problem.[13,14] Our calculation combines results from Ref. 2 with boundary conditions that arise at the interface of two nonlinear media. We find that the reflected SH intensity oscillates as a function of overlayer thickness. In contrast to the simple Maker fringe result, however, more than six Fourier components contribute to the spatial dependence of this oscillation. Finally, we use our interference data along with our theoretical solution to determine the frequency dependence of the bulk second-order susceptibility of ZnSe.

The remainder of the paper is organized as follows. We first describe the experimental apparatus and our samples. Then we present theoretical calculations of the nonlinear interference effect, and compare these calculations with experiment. Finally, we present measurements of the frequency dependence of the ZnSe and GaAs bulk second-order nonlinearities as a function of the SH photon energy between 2.6 and 3.1 eV.

II. EXPERIMENT

Our heterostructure sample consists of an epitaxial layer of undoped ($n \leq 1 \times 10^{15}$ cm^{-3}) ZnSe(001), with thickness ranging from 50 Å to 1 μm, grown on a 0.5-

μm undoped ($n \leq 5 \times 10^{15}$ cm^{-3}) GaAs film terminated with 2×4 surface reconstruction. The films were grown by molecular-beam epitaxy (MBE) on an n^+ silicon-doped GaAs substrate in a dual MBE chamber, according to procedures previously described.[7] At present there is substantial technological interest in the ZnSe/GaAs heterostructure, because ZnSe has been demonstrated to lase near its optical band-gap energy of ~2.7 eV.[15] As a result of this interest our samples have been well characterized morphologically, chemically, and to some extent electrically.[16]

A schematic of the experimental apparatus is shown in Fig. 1. The SHG spectra for each sample were obtained by irradiating the sample with light from a Nd-YAG (yttrium-aluminum-garnet) pumped tunable dye laser, and the power of the reflected light at the second-harmonic frequency was measured as a function of wavelength. The incident light pulses were collimated to be ~1.5 mm in diameter, had a temporal duration of 9 nsec, and a fluence of ~5 mJ/cm^2. Typical SHG signals were ~50 photons/pulse. An angle of incidence of 75° was used in all experiments. At this angle > 50% of the fundamental light was transmitted into the ZnSe overlayer.

In order to compensate for intensity fluctuations of the input beam and systematics in our detection system, a SH signal was simultaneously produced and measured in transmission along a parallel (reference) optical path containing a wedged quartz plate with 0.8° apex angle. The maximum SH power of the reference at each frequency was obtained by translating the wedged quartz along a direction perpendicular to the laser-beam propagation vector. Our sample intensities were normalized using this reference SHG signal.

The bulk signals from the ZnSe/GaAs(001) samples were separated from the interface signals by proper choice of sample orientation and light polarization.[17] GaAs and ZnSe are zinc-blende crystals with $\bar{4}3m$ symmetry. They both have a single nonzero bulk second-order susceptibility tensor element, $\vec{\chi}^{(2)}_{xyz}$,[18] whose contribution to the output radiation is highly anisotropic. For the p-in–s-out polarization configuration, the SHG output intensity is proportional to $\cos^2(2\phi)$, where ϕ is the angle between

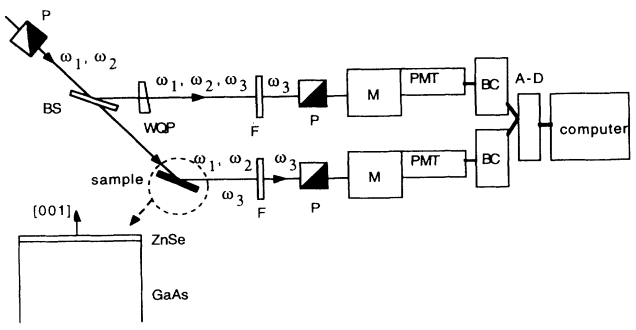

FIG. 1. Schematic of experimental setup: P, polarizer; F, spectral filter; PMT, photomultiplier tube; M, monochromator; BC, boxcar averager; WQP, wedged quartz plate; BS, beam splitter; A-D, analog-to-digital converter.

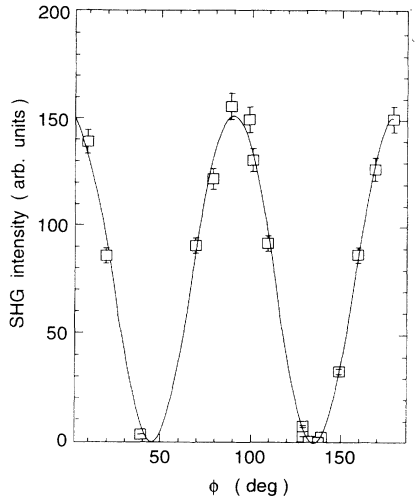

FIG. 2. Reflected SHG intensity at fixed frequency from the ZnSe/GaAs(001) crystal as a function of the rotation angle ϕ (degrees). Here ϕ is the angle between the [100] direction and the plane of incidence. The input is p polarized and the output is s polarized. The ratio of the peak signal to null signal is $\geq$ 5000. The solid line is a theoretical prediction for this signal variation.

the [100] direction and the plane of incidence. The orientation dependence of our SHG signal is illustrated in Fig. 2. Frequency-dependent measurements were performed using the p-in–s-out polarization configuration at $\phi = 0$. Using this configuration we maximized our sensitivity to the bulk nonlinearity. In analyzing our results we have used the linear dielectric constants for GaAs and ZnSe given in Refs. 19 and 20, respectively. These values were checked against our own linear reflectivity measurements and agreement was good.

III. THEORY

In this section we review the theoretical aspects of the reflected SH from a semi-infinite medium,[2] and then we develop a full theoretical expression for the reflected SH field of two adjoined nonlinear slabs. Because our experiments utilized the p-in–s-out polarization configuration, calculation for p-in–s-out polarization will be given in detail. Calculation for the s-in–p-out and p-in–p-out polarization configurations are straightforward extensions of the p-in–s-out results.

For all the expressions below, the subscripts "0," "1," and "2" refer to vacuum, first medium, and second medium, respectively. The subscript "1" is also used for the semi-infinite medium. The subscript "Rlm" refers to the reflected harmonic wave which is generated in medium "l" and propagates through medium "m." We also assume that the second-order susceptibilities and dielectric constants change discontinuously at all interfaces.

A. Review of semi-infinite medium results

In the semi-infinite problem, solved by Bloembergen and Pershan,[2] a monochromatic plane wave with fre-

quency ω impinges from vacuum onto a crystal that lacks inversion symmetry. The incident wave is refracted into the crystal, and the transmitted field interacts with the nonlinear medium to produce a second-harmonic source polarization, $\mathbf{P}^{(2\omega)}$. The source polarization radiates an electromagnetic wave with angular frequency 2ω. The propagation of the radiated second-harmonic electric field, $\mathbf{E}^{(2\omega)}$, must obey the nonlinear wave equation,

$$\nabla \times \nabla \times \mathbf{E}^{(2\omega)} + \frac{\epsilon(2\omega)}{c^2}\frac{\partial^2}{\partial t^2}\mathbf{E}^{(2\omega)} = -\frac{4\pi}{c^2}\frac{\partial^2}{\partial t^2}\mathbf{P}^{(2\omega)}, \tag{1}$$

where $\epsilon(\omega)$ is the ω-dependent linear dielectric constant of the semi-infinite medium, and the source polarization is given by

$$\mathbf{P}^{(2\omega)} = \overleftrightarrow{\chi}^{(2)} : \mathbf{E}_t^{(\omega)}\mathbf{E}_t^{(\omega)} e^{i(\mathbf{k}_b \cdot \mathbf{r} - 2\omega t)}. \tag{2}$$

Here $\overleftrightarrow{\chi}^{(2)}$ represents the second-order nonlinear susceptibility tensor of the crystal, and $\mathbf{E}_t^{(\omega)}$ represents the transmitted fundamental field with the wave vector $\mathbf{k}_t$, and $\mathbf{k}_b = 2\,\mathbf{k}_t$.

We choose the coordinate system so that the vacuum-crystal boundary is at $z = 0$, and the plane of incidence contains the z and x axis [Fig. 3(a)]. If $\overleftrightarrow{\chi}^{(2)}$ is independent of position inside the semi-infinite medium, the exact solution to Eq. (1) is

$$\mathbf{E}^{(2\omega)} = \mathbf{E}_f^{(2\omega)} e^{i(\mathbf{k}_f \cdot \mathbf{r} - 2\omega t)} - \frac{4\pi(4\omega^2/c^2)P}{k_f^2 - k_b^2}\left[\hat{\mathbf{p}} - \frac{\mathbf{k}_b(\mathbf{k}_b \cdot \hat{\mathbf{p}})}{k_f^2}\right] e^{i(\mathbf{k}_b \cdot \mathbf{r} - 2\omega t)}, \tag{3}$$

where $\hat{\mathbf{p}}$ is a unit vector in the direction of $\mathbf{P}^{(2\omega)}$. The first term of Eq. (3) is the free wave solution. This wave propagates in the direction of $\mathbf{k}_f$, and its amplitude is determined by boundary conditions. The second term is a particular solution of the nonlinear wave equation. This field is *bound* to the fundamental wave, and propagates with wave vector $\mathbf{k}_b$. The magnitude of the free (bound) wave vector in medium i is represented by $\mathbf{k}_{fi}$ ($\mathbf{k}_{bi}$).

A harmonic wave $\mathbf{E}_{R10}^{(2\omega)}$ is also radiated into the vacuum. The wave vector of this reflected SH, $\mathbf{k}_{f0}$, has the same direction as the reflected fundamental field. The s-polarized component of $\mathbf{E}_{R10}^{(2\omega)}$, i.e., $E_{\perp,R10}^{(2\omega)}$, is proportional to the component of P along the y axis in medium 1, $P_{\perp,1}$, i.e.,

$$E_{\perp,R10}^{(2\omega)} = \frac{4\pi P_{\perp,1}}{\epsilon_{b1} - \epsilon_{f1}}\left[\frac{k_{f1,z} - k_{b1,z}}{k_{f1,z} - k_{f0,z}}\right]. \tag{4}$$

Here, $k_{ij,z}$ is the z component of $\mathbf{k}_{ij}$ and $\epsilon_{bj}(2\omega) = \epsilon_j(\omega)$, $\epsilon_{fj}(2\omega) = \epsilon_j(2\omega)$, and $\epsilon_j(\omega)$ is the ω-dependent linear dielectric constant of medium j. Conservation of $k_{\|}$ at all frequencies (Snell's law) enables one to determine the components of each wave vector as a function of the incident wave vector.

For zinc-blende crystals such as GaAs(001) and ZnSe(001) in the p-in–s-out polarization configuration, the second-order bulk polarization has the form

$$P_{\perp,1}^{(2\omega)} = \frac{-k_{t1,z}\,k_{t1,x}}{k_{t1}^2} 2\cos(2\phi)\, t_{\|,01}^{(\omega)2}\, \overleftrightarrow{\chi}_{xyz}^{(2)}\, E_{\|}^{(\omega)2}, \tag{5}$$

where $t_{\alpha,ij}^{(\omega)}$ ($r_{\alpha,ij}^{(\omega)}$) is the Fresnel refraction (reflection) coefficient for an α-polarized light beam with angular frequency ω propagating from medium i to medium j, and $E_{\|}^{(\omega)}$ is the component of the incident p-polarized input field parallel to the plane of incidence. $k_{t1,z}$ and $k_{t1,x}$ are the z and x wave vector components, respectively, of the transmitted fundamental field in medium 1. Using Eqs. (4) and (5) we have

$$E_{\perp,R10}^{(2\omega)} = \overleftrightarrow{\chi}_{xyz}^{(2)}\, Y\, E_{\|}^{(\omega)2}, \tag{6}$$

where

$$Y = \frac{-k_{t1,z}\,k_{t1,x}}{k_{t1}^2}\,\frac{4\pi}{\epsilon_{b1} - \epsilon_{f1}}\,\frac{k_{f1,z} - k_{b1,z}}{k_{f1,z} - k_{f0,z}}\, 2\cos(2\phi)\, t_{\|,01}^{(\omega)2}. \tag{7}$$

The coefficient Y depends only on the linear properties of the bulk medium and can be calculated. Using a calculated Y and measured $|\mathbf{E}_{\perp,R10}^{(2\omega)}|^2$ we can determine $|\overleftrightarrow{\chi}_{xyz}^{(2)}|$. In Fig. 4 we plot measured values of $|\mathbf{E}_{\perp,R10}^{(2\omega)}|^2$ and $|\overleftrightarrow{\chi}_{xyz}^{(2)}|$ for GaAs(001).

In some physical situations the magnitude of the second-order susceptibility can vary as a function of po-

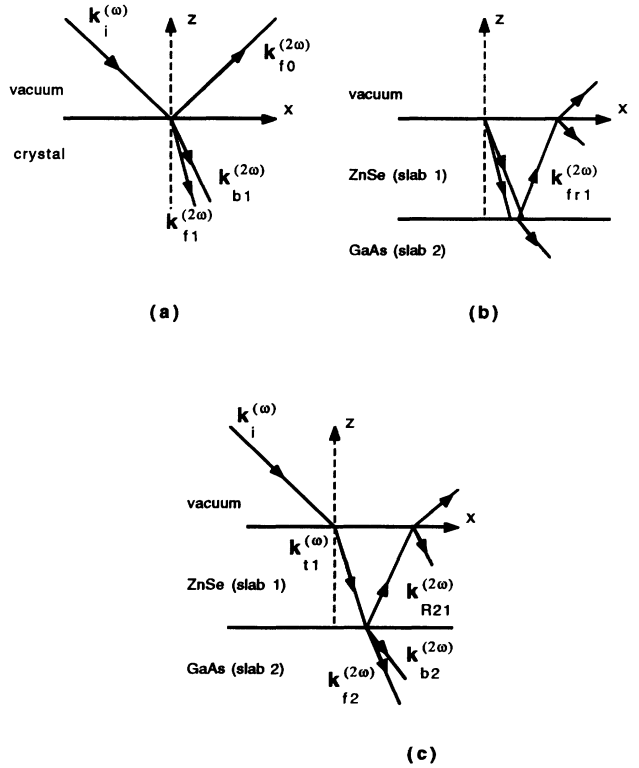

FIG. 3. Simplified coordinate system that defines the boundaries and the direction of the fundamental and second-harmonic electric fields for the case of the semi-infinite slab (a), and the two-slab problem (b) and (c). All angles between the wave vectors and z axis are positive and less than 90°.

sition within the semi-infinite medium. This can arise as a result of local stresses or electric fields near the interface. In Appendix A we give a solution for the special case where the susceptibility decays exponentially with distance from the vacuum-crystal interface.

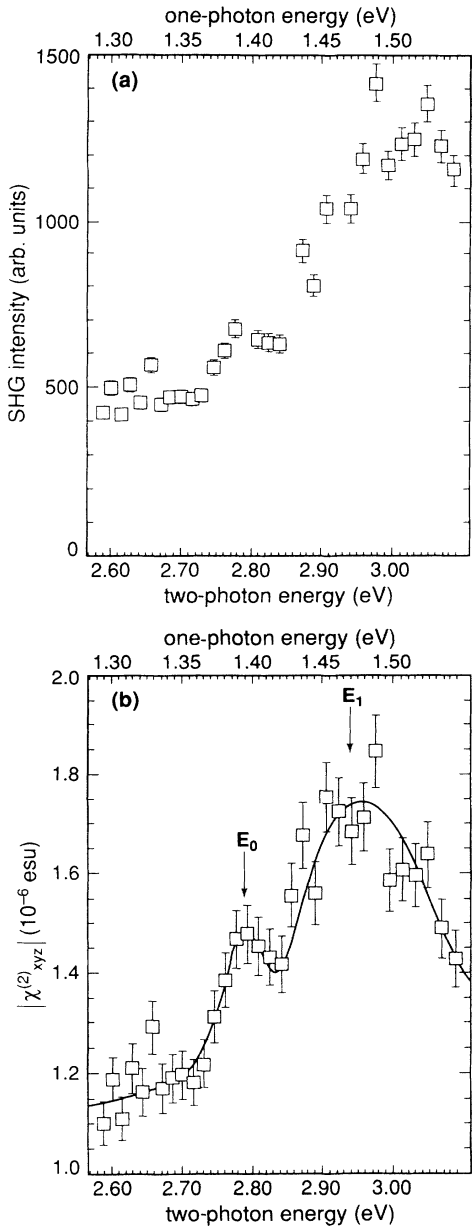

FIG. 4. (a) Normalized bulk SHG intensity of GaAs(001) as a function of one- and two-photon energy. The error bars represent the full range of values obtained from several measurements. (b) $|\chi^{(2)}_{xyz}|$ as a function of one- and two-photon energy for GaAs derived from the data in (a) using Eq. (7). The E_1 and E_0 peaks correspond to two- and one-photon resonances at ~2.96 and ~1.4 eV, respectively. The solid line is only a guide for the eye. In order to deduce the second-order susceptibility of our sample, the SH output power of the reference wedged quartz was measured, and the effects of the finite beam waist in the quartz crystal were included in the calculation to determine $|\vec{\chi}^{(2)}_{xyz}|$.

B. Two adjoined nonlinear optical slabs

The second-harmonic field produced in reflection from two nonlinear slabs is more complex. This complexity arises as a result of the additional interface and the second nonlinear medium. There are a number of existing schemes that can be used to compute our result.[13,14] The matrix methods[13,14] are particularly useful for problems with many layers, and can be applied here as well. We will continue, however, to use the results of Ref. 2, in combination with more conventional results from linear optics. Loosely speaking, there are three fields which contribute to the total reflected second-harmonic field in the vacuum: (1) a reflected SH field generated from the first slab, (2) a multiply reflected SH field produced as a result of the propagation of the free and bound harmonic waves in medium 1, and (3) a multiply reflected SH field generated from the second slab. We will see that the total reflected SH intensity in the vacuum oscillates with respect to overlayer thickness at spatial frequencies determined by $k_{f1,z}$, $k_{b1,z}$, and $k_{b2,z}$.

The first reflected SH field is produced in slab 1 and propagates into the vacuum in the direction of the fundamental reflected field [Fig. 3(a)]. The solution for this wave is given by Eq. (6) with values of $\vec{\chi}^{(2)}$ and Y appropriate to medium 1, which in our case is ZnSe(001).

The second field [depicted in Fig. 3(b)] is produced when both free and bound waves generated in medium 1 propagate to the buried interface at $z = -d$. Their propagation obeys Eq. (3). In general, both bound and free waves are reflected from the interface. The exact boundary conditions used to determine these fields are given in Appendix B. The reflection of the bound wave depends primarily on the linear reflection of the fundamental wave at the buried interface. If the reflection amplitude for the fundamental field is small, the reflected bound wave is also small and our solution simplifies. This is the case for the ZnSe/GaAs(001) interface in our measured energy range. The reflected fundamental intensity is at least 20 times smaller than the incident fundamental intensity, and we safely use the simpler result to find that

$$E^{(2\omega)}_{\perp,R11} = r^{(2\omega)}_{\perp,12} E_{f1} e^{-2idk_{f1,z}} + \left[\frac{k_{b1,z} - k_{f2,z}}{k_{f1,z} + k_{f2,z}}\right] \frac{4\pi P_{\perp,1}}{\epsilon_{b1} - \epsilon_{f1}} e^{-id(k_{f1,z}+k_{b1,z})}. \quad (8)$$

This field propagates to the first boundary at $z = 0$ where some harmonic light is transmitted into the vacuum. Multiple reflections change the amplitude of the transmitted field by a factor of

$$g = \left[1 - r^{(2\omega)}_{\perp,10} r^{(2\omega)}_{\perp,12} e^{-2idk_{f1,z}}\right]^{-1}. \quad (9)$$

The effects of multiple reflections are important for thin overlayers, and must be included to ensure that radiation from medium 1 reduces to zero as the first slab thickness approaches zero.

A third SH field is depicted in Fig. 3(c), and discussed in detail in Appendix B. It arises when the fundamental

field is transmitted through medium 1 into medium 2. In medium 2 the field interacts to produce a nonlinear polarization, $\mathbf{P}_{\perp,2}^{(2\omega)}$. This polarization radiates a field back into medium 1 given by Eq. (6). In our case we must insert values of $\overleftrightarrow{\chi}_{xyz}^{(2)}$ and Y appropriate to GaAs(001) and the ZnSe/GaAs(001) interface. The reflected second-harmonic wave due to the second slab $E_{\perp,R21}^{(2\omega)}$ is

$$E_{\perp,R21}^{(2\omega)} = \frac{4\pi P_{\perp,2}}{\epsilon_{b2} - \epsilon_{f2}} \left[\frac{k_{f2,z} - k_{b2,z}}{k_{f1,z} + k_{f2,z}} \right] e^{-id(k_{f1,z}+k_{b2,z})}. \tag{10}$$

This field propagates to the first interface at $z = 0$ where again some light at 2ω is transmitted into the vacuum. Multiple reflections also change the amplitude of this field by a factor of g. The total reflected field is the sum of all harmonic fields in the vacuum. This field can be written in a fairly simple form that clearly delineates the linear and nonlinear contribution of the two layers,

$$E_{\perp,\mathrm{tot}}^{(2\omega)} = (Y_1 \overleftrightarrow{\chi}_{xyz-1}^{(2)} + Y_2 \overleftrightarrow{\chi}_{xyz-2}^{(2)}) E_{\parallel}^{(\omega)2}. \tag{11}$$

Here,

$$Y_1 = g t_{\perp,10}^{(2\omega)} Q_1 \left[r_{\perp,12}^{(2\omega)} \left(\frac{k_{f0,z} - k_{b1,z}}{k_{f1,z} - k_{f0,z}} \right) e^{-2idk_{f1,z}} + \left(\frac{k_{b1,z} - k_{f2,z}}{k_{f1,z} + k_{f2,z}} \right) e^{-id(k_{f1,z}+k_{b1,z})} + \frac{1}{g t_{\perp,10}^{(2\omega)}} \left(\frac{k_{b1,z} - k_{f1,z}}{k_{f0,z} - k_{f1,z}} \right) \right], \tag{12}$$

$$Y_2 = g t_{\parallel,12}^{(\omega)2} t_{\perp,10}^{(2\omega)} Q_2 \left[\frac{k_{f2,z} - k_{b2,z}}{k_{f2,z} + k_{f1,z}} \right] e^{-id(k_{f1,z}+k_{b2,z})}, \tag{13}$$

$$Q_j = \frac{4\pi t_{\parallel,01}^{(\omega)2}}{\epsilon_{bj} - \epsilon_{fj}} \frac{-k_{tj,z} k_{tj,x}}{k_{tj}^2} 2\cos(2\phi), \tag{14}$$

and the detected harmonic intensity $I_{\mathrm{tot}}^{(2\omega)}$ is

$$I_{\mathrm{tot}}^{(2\omega)} = \frac{c}{8\pi} |E_{\perp,\mathrm{tot}}^{(2\omega)}|^2. \tag{15}$$

The Y_i depend on overlayer thickness d, incidence angle, and various constants that are derived from the linear properties of the media. This function is a complex exponential and is responsible for the oscillation of the intensity of the total reflected SH field and the decay of the SH power with increasing overlayer thickness.

The intensity of $E_{\perp,\mathrm{tot}}$, without multiple reflections, contains six oscillatory terms of the form $\sin^2(d(k_{f1,z} \pm k_{\beta,z})/2)$ and $\sin^2(d(k_{b1,z} - k_{b2,z})/2)$, where $\beta = b1$, $b2$, and $f1$. This is to be contrasted with the Maker fringe result, which has only one oscillatory term when multiple reflections are omitted, i.e., $\sin^2(d(k_{f1,z} - k_{b1,z})/2)$. The number of oscillatory terms *increases* when multiple reflections are included. None of the differences discussed above arise unless the second-order susceptibility in the second slab is nonzero.

IV. RESULTS

We have measured the SHG spectra of nine ZnSe/GaAs(001) samples with different overlayer thicknesses (Fig. 5). In this way we determined the thickness dependence of the reflected SH intensity at various photon energies. The result at 2.67 eV is shown in Fig. 6. The intensity shows a strong oscillation with respect to the thickness of the overlayer. For large values of the thickness, d, the intensity approaches the SH intensity of a semi-infinite slab of ZnSe. We have observed this two-slab interference effect for SH photon energies between 2.6 and 3.1 eV.

The second-order susceptibility of GaAs(001) deduced from our separate SHG measurements, along with literature values for the dielectric constants of ZnSe and GaAs, were used to fit each set of interference data to Eqs. (11)–(15). The solid line in Fig. 6 is a theoretical fit to our

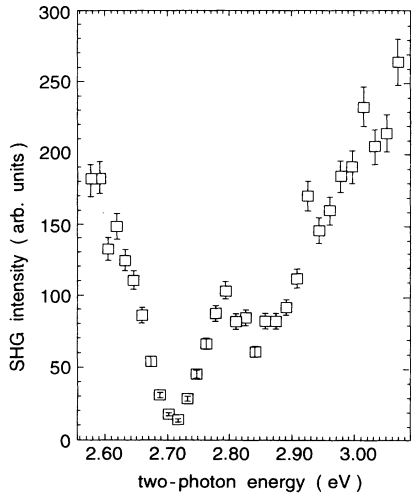

FIG. 5. Normalized SH intensity signals from the bulk of our ZnSe/GaAs(001) sample as a function of two-photon energy. The ZnSe overlayer thickness was 250 Å. The error bars represent the full range of values obtained from several measurements.

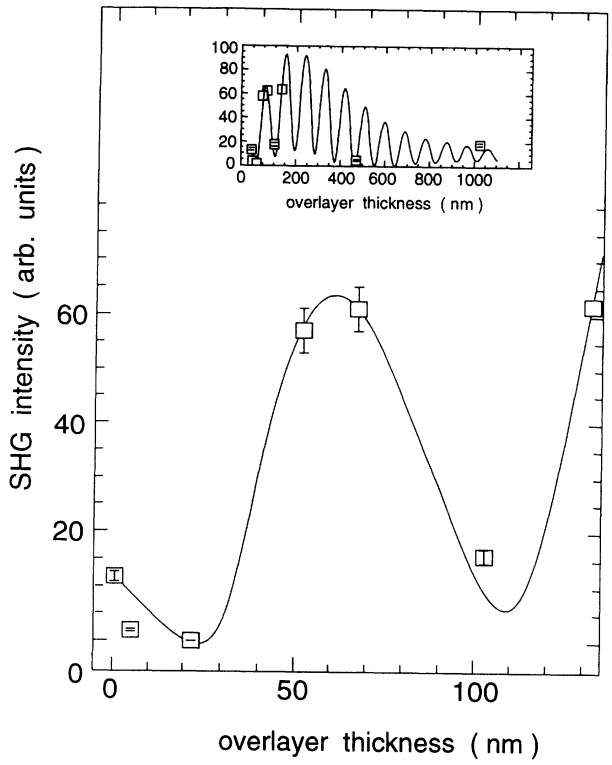

FIG. 6. Variation of the normalized SH intensity reflected from ZnSe/GaAs(001) as a function of the overlayer thickness at 2.67 eV. The solid line is a theoretical fit using Eqs. (11)–(15). The lower portion of the figure is a reproduction of the overlayer data for a smaller range of thicknesses.

experimental data. The agreement is good. It lends support for our assumption that the second-order bulk susceptibility of our samples is independent of position in each medium within the sample, and it corroborates our primary theoretical results.

The magnitude of the second-order susceptibility of ZnSe, and its relative phase with respect to $\vec{\chi}^{(2)}_{xyz}$ of GaAs, were the only two free parameters in our fitting routine. Thus we are able to use our interference data to deduce the frequency-dependent magnitude of the second-order susceptibility of ZnSe. Our deduced $|\vec{\chi}^{(2)}_{xyz}|$ for ZnSe are shown in Fig. 7(a). This susceptibility exhibits a relatively sharp resonance at ~2.67 eV. This peak corresponds to the E_0 transition of ZnSe. In addition, we see that the phase between the ZnSe and GaAs susceptibilities changes by 180° near this resonance [Fig. 7(b)]. The E_0 transition of GaAs is also responsible for the small peak at 1.4 eV shown in Fig. 4. The GaAs peak is less pronounced than the ZnSe because the joint density of states (JDOS) at the Γ point in GaAs is ~20 times smaller than in ZnSe.[21] Previous measurements of $\vec{\chi}^{(2)}_{xyz}$ in GaAs (Refs. 22–25) did not exhibit the E_0 transition of this semiconductor. This may have been a result of poor resolution of the apparatus and/or sample quality. The broad peak at ~2.96 eV in Fig. 4 corresponds to the E_1 transition of GaAs.

V. CONCLUSION

We have reported the observation of a class of interference phenomena that arises in reflected SHG from two physically adjoined nonlinear slabs. A theoretical expres-

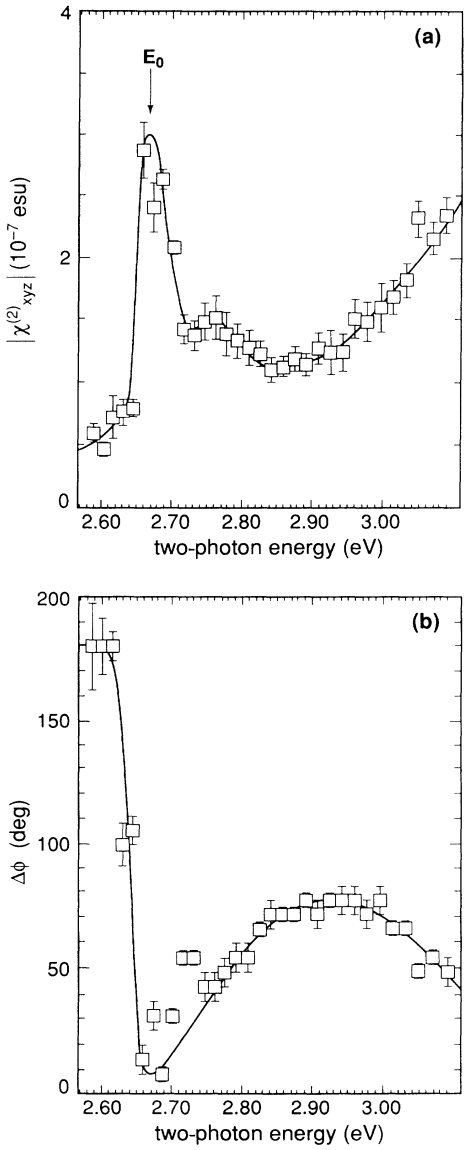

FIG. 7. (a) Magnitude of the second-order susceptibility of the bulk of ZnSe(001) for energies between 2.6 and 3.1 eV. (b) The relative phase of ZnSe susceptibility with respect to $\vec{\chi}^{(2)}_{xyz}$ of GaAs. The error bars were derived from the fits by standard statistical methods. Uncertainties in the second-order susceptibility of GaAs introduced a small additional uncertainty in the reported ZnSe susceptibility and phase, but this uncertainty was much smaller than the errors reported above. The solid lines are only a guide for the eye.

sion for this phenomenon was derived and used to fit the data. This interference phenomenon was then used to deduce the *frequency-dependent* second-order bulk susceptibility of the overlayer slab. The $|\vec{\chi}^{(2)}_{xyz}|$ of ZnSe exhibits a sharp resonance at 2.67 eV which we have assigned to the E_0 transition in ZnSe. The frequency dependence of $|\vec{\chi}^{(2)}_{xyz}|$ in GaAs was also measured in the same spectral region, and the E_0 and E_1 transitions of GaAs were observed.

ACKNOWLEDGMENTS

We would like to thank E. Burstein and S. Rabii for stimulating discussions, and A. Denenstein for valuable technical help. This work was supported by the ONR through Contract No. N00014-91-J-1867. A.G.Y. also acknowledges partial support from Petroleum Research Fund through Grant No. PRF22328-GS, the National Science Foundation through the PYI program No. DMR-9058498 and the MRL program Grant No. DMR-8519059, and the Alfred P. Sloan Foundation.

APPENDIX A: SOLUTION OF THE NONLINEAR WAVE EQUATION WITH POSITION-DEPENDENT $\vec{\chi}^{(2)}$

Localized electric fields or deformation potentials can make $\vec{\chi}^{(2)}$ position dependent. If the second-order susceptibility tensor $\vec{\chi}^{(2)}$ decays exponentially in the direction of $\hat{\mathbf{z}}$ with decay constant α, we can write the position-dependent polarization $P^{(2\omega)}$ as

$$P = P_0 e^{-\alpha(z+d)}, \tag{A1}$$

where P_0 is the polarization at the interface $z = -d$. Then, assuming the linear dielectric constant is still independent of position, the nonlinear wave equation (1) has a solution of the form (3), but with a modified $\mathbf{k}_b$,

$$\mathbf{k}_b = 2\mathbf{k}_t + i\alpha\hat{\mathbf{z}}. \tag{A2}$$

This leads to a new form for $\epsilon_b(2\omega)$,

$$\epsilon_b(2\omega) = \epsilon(\omega) + \frac{c^2}{4\omega^2}\left(4i\alpha\mathbf{k}_t\cdot\hat{\mathbf{z}} - \alpha^2\right). \tag{A3}$$

Thus the polarization decay indirectly affects the free wave propagation through the boundary conditions, and of course, it directly affects the bound wave amplitude in the $\hat{\mathbf{z}}$ direction.

APPENDIX B: EXACT BOUNDARY CONDITIONS AT BURIED INTERFACE

To solve the general problem of reflection at the boundary between two nonlinear media, we look for solutions on *both sides* of the interface in the form of Eq. (3). The general boundary conditions in the p-in–s-out polarization configuration at the buried interface, which include the nonlinearity of both slabs, can be written as follows:

(a) Continuity of $E_{\parallel}$,

$$E_{f1}\,e^{i\mathbf{k}_{f1}\cdot\mathbf{r}_o} + \frac{4\pi P_{\perp,1}}{\epsilon_{b1}-\epsilon_{f1}}\,e^{i\mathbf{k}_{b1}\cdot\mathbf{r}_o} + E_{fr}\,e^{i\mathbf{k}_{fr1}\cdot\mathbf{r}_o} + \frac{4\pi P'_{\perp,1}}{\epsilon_{b1}-\epsilon_{f1}}\,e^{i\mathbf{k}_{br1}\cdot\mathbf{r}_o} = E_{f2}\,e^{i\mathbf{k}_{f2}\cdot\mathbf{r}_o} + \frac{4\pi P_{\perp,2}}{\epsilon_{b2}-\epsilon_{f2}}\,e^{i\mathbf{k}_{b2}\cdot\mathbf{r}_o}; \tag{B1}$$

(b) continuity of $H_{\parallel}$,

$$E_{f1}k_{f1,z}\,e^{i\mathbf{k}_{f1}\cdot\mathbf{r}_o} + \frac{4\pi P_{\perp,1}}{\epsilon_{b1}-\epsilon_{f1}}k_{b1,z}\,e^{i\mathbf{k}_{b1}\cdot\mathbf{r}_o} - E_{fr}k_{f1,z}\,e^{i\mathbf{k}_{fr1}\cdot\mathbf{r}_o} - \frac{4\pi P'_{\perp,1}}{\epsilon_{b1}-\epsilon_{f1}}k_{b1,z}\,e^{i\mathbf{k}_{br1}\cdot\mathbf{r}_o}$$

$$= E_{f2}k_{f2,z}\,e^{i\mathbf{k}_{f2}\cdot\mathbf{r}_o} + \frac{4\pi P_{\perp,2}}{\epsilon_{b2}-\epsilon_{f2}}k_{b2,z}\,e^{i\mathbf{k}_{b2}\cdot\mathbf{r}_o}. \tag{B2}$$

Here the reflected bound wave amplitude is proportional to $P'_{\perp,1}$, and

$$P'_{\perp,1} = r^{(\omega)2}_{\parallel,12}P_{\perp,1}. \tag{B3}$$

k_{fr1} and k_{br1} are wave vectors of the reflected free and bound wave in medium 1, respectively, and $\mathbf{r}_o$ is the position vector at the interface. E_{fr} (E_{ft}) is the amplitude of the reflected (refracted) free wave at 2ω. The relation between E_{fr} and the reflected SH fields in the main text, i.e., $E_{\perp,R11}$ and $E_{\perp,R21}$, is further clarified below.

Equations (B1)–(B3) lead to the determination of E_{fr}:

$$E_{fr} = r^{(2\omega)}_{\perp,12}E_{f1}\,e^{-2idk_{f1,z}} + \left[\frac{k_{b1,z}-k_{f2,z}}{k_{f1,z}+k_{f2,z}}\right]\frac{4\pi P_{\perp,1}}{\epsilon_{b1}-\epsilon_{f1}}\left[1+\frac{k_{f2,z}+k_{b1,z}}{k_{f2,z}-k_{b1,z}}\,r^{(\omega)2}_{\parallel,12}\,e^{i2dk_{b1,z}}\right]e^{-id(k_{f1,z}+k_{b1,z})}$$
$$+\frac{4\pi P_{\perp,2}}{\epsilon_{b2}-\epsilon_{f2}}\left[\frac{k_{f2,z}-k_{b2,z}}{k_{f1,z}+k_{f2,z}}\right]e^{-id(k_{f1,z}+k_{b2,z})}. \tag{B4}$$

The reflected SH field, $E_{\perp,R11}$, arises from the first and second terms of (B4). The third term in (B4) gives rise to $E_{\perp,R21}$ of the main text. We can see how these terms arise by building up our solution from two separate boundary value problems. In the first problem we suppress the nonlinearity of the second slab. In this case $P_{\perp,2} = 0$ in Eq. (B4), and all harmonic waves originate from the first slab. In the second problem we ignore the harmonic waves generated in the first slab and study the effect of the nonlinearity of the second slab. In this case E_{f1} and $P_{\perp,1}$ are zero in Eq. (B4). The total solution is, of course, a superposition of these resulting fields.

The solution to the boundary conditions is algebraically simpler if the reflection of the fundamental field at the buried interface is small, i.e.,

$$r_{\parallel,12}^{(\omega)2} \ll 1. \tag{B5}$$

Under these circumstances we can ignore both the reflected bound wave and the effect of this field on the reflected free wave, E_{fr}. This leads to the following simplifications for $E_{\perp,R11}$, $P'_{\perp,1}$, and $E_{\perp,R21}$:

$$E_{\perp,R11}^{(2\omega)} = r_{\perp,12}^{(2\omega)} E_{f1}\, e^{-2idk_{f1,z}} + \left[\frac{k_{b1,z} - k_{f2,z}}{k_{f1,z} + k_{f2,z}}\right] \frac{4\pi P_{\perp,1}}{\epsilon_{b1} - \epsilon_{f1}} e^{-id(k_{f1,z}+k_{b1,z})}, \tag{B6}$$

$$P'_{\perp,1} = 0, \tag{B7}$$

$$E_{\perp,R21}^{(2\omega)} = \frac{4\pi P_{\perp,2}}{\epsilon_{b2} - \epsilon_{f2}} \left[\frac{k_{f2,z} - k_{b2,z}}{k_{f1,z} + k_{f2,z}}\right] e^{id(k_{f1,z}-k_{b2,z})}. \tag{B8}$$

The condition (B5) exists for our ZnSe/GaAs(001) samples, and the small correction is not included in the results presented in the main text. The expressions (B6) –(B8) can also be derived from a more general N-layer result presented in Ref. 13. In order to obtain (B6) – (B8) it is necessary to convert the general expression in Ref. 13 to the p-in–s-out polarization configuration, and then apply the boundary conditions (B1) and (B2) with $P'_{\perp,1} = 0$ to the general solutions.

[1] M. Born and E. Wolf, *Principles of Optics* (Pergamon, Oxford, 1975).
[2] N. Bloembergen and P. S. Pershan, Phys. Rev. **128**, 606 (1962).
[3] P. D. Maker, R. W. Terhune, M. Nisenoff, and C. M. Savage, Phys. Rev. Lett. **8**, 21 (1962).
[4] J. Jerphagnon and S. K. Kurtz, J. Appl. Phys. **41**, 1667 (1970).
[5] See, for example, G. Berkovic, Y. R. Shen, G. Marowsky, and R. Steinhoff, J. Opt. Soc. Am. B **6**, 205 (1989), and references therein.
[6] G. A. Reider, A. J. Schmidt, and G. Marowsky, Opt. Commun. **47**, 223 (1983).
[7] For details of sample growth and morphology, see M. C. Tamargo, J. L. deMiguel, D. M. Hwang, and H. H. Farrell, J. Vac. Sci. Technol. B **6**, 784 (1988), and references therein.
[8] E. Ghahramani, D. J. Moss, and J. E. Sipe, Phys. Rev. Lett. **64**, 2815 (1990).
[9] T. F. Heinz, F. J. Himpsel, E. Palange, and E. Burstein, Phys. Rev. Lett. **63**, 644 (1989).
[10] J. F. McGilp and Y. Yeh, Solid State Commun. **59**, 91 (1986).
[11] M. S. Yeganeh, A. G. Yodh, and M. C. Tamargo, in *Quantum Electronics and Laser Science, 1991,* Technical Digest Series Vol. 11 (Optical Society of America, Washington, D.C., 1991), p. 30; J. C. Hamilton, R. T. Tung, and H. W. K. Tom, *ibid.*
[12] M. S. Yeganeh, J. Qi, A. G. Yodh, and M. C. Tamargo, Phys. Rev. Lett. **68**, 3761 (1992).
[13] D. S. Bethune, J. Opt. Soc. Am. B **8**, 367 (1991); **6**, 910 (1989).
[14] Y. R. Shen and F. Demartini, in *Surface Polaritons*, edited by W. M. Agranovich and D. L. Mills (North-Holland, Amsterdam, 1982).
[15] M. A. Haase, J. Qiu, J. M. Depuydt, and H. Cheng, Appl. Phys. Lett. **59**, 1272 (1991).
[16] M. C. Tamargo, R. E. Nahory, B. J. Skromme, S. M. Shibli, A. L. Weaver, R. J. Martine, and H. H. Farrell, J. Cryst. Growth **111**, 741 (1991).
[17] T. Stehlin, M. Feller, P. Guyot-Sionnest, and Y. R. Shen, Opt. Lett. **13**, 389 (1988).
[18] Y. R. Shen, *The Principles of Nonlinear Optics* (Wiley-Interscience, New York, 1984).
[19] B. O. Seraphin and H. E. Bennett, *Semiconductors and Semimetals* (Academic, New York, 1967), Vol. 3.
[20] M. Aven, D. T. F. Marple, and B. Segall, J. Appl. Phys. **32**, 2261 (1961).
[21] This can be seen from the relation JDOS $\propto \mathrm{Im}(\epsilon)\, E^2$. Here, E is the energy and $\mathrm{Im}(\epsilon)$ is the imaginary part of the dielectric constant at energy E. For further details on this point see M. Cardona and D. L. Greenaway, Phys. Rev. **133**, A1685 (1964), or M. Cardona, *Modulation Spectroscopy* (Academic, New York, 1969).
[22] H. Lotem, G. Koren, and Y. Yacoby, Phys. Rev. B **9**, 3532 (1974).
[23] D. Bethune, A. J. Schmidt, and Y. R. Shen, Phys. Rev. B **11**, 3867 (1975).
[24] R. K. Chang, J. Ducuing, and N. Bloembergen, Phys. Rev. Lett. **15**, 415 (1965).
[25] F. G. Parsons and R. K. Chang, Opt. Commun. **3**, 173 (1971).

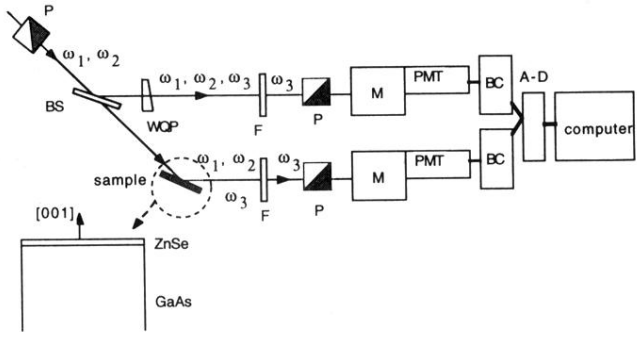

FIG. 1. Schematic of experimental setup: P, polarizer; F, spectral filter; PMT, photomultiplier tube; M, monochromator; BC, boxcar averager; WQP, wedged quartz plate; BS, beam splitter; A-D, analog-to-digital converter.